





3 | Bacteriology | Research Article

# Pseudomonas aeruginosa surface motility and invasion into competing communities enhance interspecies antagonism

Andrea Sánchez-Peña, 1 James B. Winans, 2 Carey D. Nadell, 2 Dominique H. Limoli 1,3

**AUTHOR AFFILIATIONS** See affiliation list on p. 15.

ABSTRACT Chronic polymicrobial infections involving Pseudomonas aeruginosa and Staphylococcus aureus are prevalent, difficult to eradicate, and associated with poor health outcomes. Therefore, understanding interactions between these pathogens is important to inform improved treatment development. We previously demonstrated that P. aeruginosa is attracted to S. aureus using type IV pili (TFP)-mediated chemotaxis, but the impact of attraction on S. aureus growth and physiology remained unknown. Using live single-cell confocal imaging to visualize microcolony structure, spatial organization, and survival of S. aureus during coculture, we found that interspecies chemotaxis provides P. aeruginosa a competitive advantage by promoting invasion into and disruption of S. aureus microcolonies. This behavior renders S. aureus susceptible to P. aeruginosa antimicrobials. Conversely, in the absence of TFP motility, P. aeruginosa cells exhibit reduced invasion of S. aureus colonies. Instead, P. aeruginosa builds a cellular barrier adjacent to S. aureus and secretes diffusible, bacteriostatic antimicrobials like 2-heptyl-4-hydroxyquinoline-N-oxide (HQNO) into the S. aureus colonies. Reduced invasion leads to the formation of denser and thicker S. aureus colonies with increased HQNO-mediated lactic acid fermentation, a physiological change that could complicate treatment strategies. Finally, we show that P. aeruginosa motility modifications of spatial structure enhance competition against S. aureus. Overall, these studies expand our understanding of how P. aeruginosa TFP-mediated interspecies chemotaxis facilitates polymicrobial interactions, highlighting the importance of spatial positioning in mixed-species communities.

**IMPORTANCE** The polymicrobial nature of many chronic infections makes their eradication challenging. Particularly, coisolation of *Pseudomonas aeruginosa* and *Staphylococcus aureus* from airways of people with cystic fibrosis and chronic wound infections is common and associated with severe clinical outcomes. The complex interplay between these pathogens is not fully understood, highlighting the need for continued research to improve management of chronic infections. Our study unveils that *P. aeruginosa* is attracted to *S. aureus*, invades into neighboring colonies, and secretes anti-staphylococcal factors into the interior of the colony. Upon inhibition of *P. aeruginosa* motility and thus invasion, *S. aureus* colony architecture changes dramatically, whereby *S. aureus* is protected from *P. aeruginosa* antagonism and responds through physiological alterations that may further hamper treatment. These studies reinforce accumulating evidence that spatial structuring can dictate community resilience and reveal that motility and chemotaxis are critical drivers of interspecies competition.

**KEYWORDS** *Pseudomonas aeruginosa, Staphylococcus aureus*, type IV pili motility, spatial organization, polymicrobial, biofilms

M icroorganisms exist in complex polymicrobial environments, such as the soil and the human body, where they interact with each other and respond to changes

**Editor** Matthew Parsek, University of Washington, Seattle, Washington, USA

Address correspondence to Dominique H. Limoli,

The authors declare no conflict of interest.

See the funding table on p. 15.

Received 2 April 2024 Accepted 2 July 2024 Published 6 August 2024

Copyright © 2024 Sánchez-Peña et al. This is an open-access article distributed under the terms of the Creative Commons Attribution 4.0 International license.

September 2024 Volume 15 Issue 9

in their surroundings (1–3). These interactions can lead to the emergence of community-level properties not observed in monoculture (4–10). The resulting collective behavior can have significant implications for the microbial physiology, evolution, and interactions with the host. For example, bacterial pathogens can enhance both virulence and antibiotic tolerance in mixed communities (2, 4, 11–16), potentially undermining current chronic infection treatments.

Pseudomonas aeruginosa and Staphylococcus aureus are the most prevalent and abundant pathogens in individuals with cystic fibrosis (CF) (5, 17) and persist in significant quantities in the lungs for decades (18). Critically, their coinfection is linked with more severe lung disease, increased rates of hospitalization, and reduced lung function in patients (19–23). Additionally, coinfection in chronic burn wounds can delay healing time (24). Thus, there is a need to further understand how interactions between these two organisms exacerbate the outcomes of polymicrobial infections.

Several in vitro studies support clinical observations that P. aeruginosa and S. aureus increase each other's virulence during coculture (12, 25). P. aeruginosa secretes numerous anti-staphylococcal factors including the siderophores pyoverdine and pyochelin, phenazines, rhamnolipids, staphylolytic proteases like LasA, and quinolones (26-32). Many of these secreted products alter S. aureus physiology, enhancing its antibiotic tolerance (13, 15, 16, 33-35). One example is the small molecule, 2-heptyl-4-hydroxyquinoline N-oxide (HQNO), which inhibits S. aureus cellular respiration, shifting its metabolism to fermentation (11, 30, 36, 37). HQNO has been detected in CF sputum (30) and can increase S. aureus tolerance to several antibiotics used clinically (13, 15, 16). However, the effect of these antimicrobials (AM) on S. aureus has been mainly studied in the presence of P. aeruginosa cell-free spent medium in a well-mixed environment (13, 15, 16, 35, 38). Interestingly, recent studies found that HQNO modifies the spatial organization of P. aeruginosa and S. aureus in a synthetic CF sputum medium (SCFM2) (39) and chronic murine wounds (40), highlighting the importance of visualizing communities in a structured environment. Therefore, to elucidate how interspecies interactions negatively impact clinical outcomes, experimental models are needed that better reflect how microbes naturally encounter each other, namely, under spatial constraint.

Previously, we demonstrated that *P. aeruginosa* responds to *S. aureus* from a distance by increasing type IV pili (TFP) motility, mediated by retractile appendages that allow *P. aeruginosa* to move across surfaces through twitching motility (41). Specifically, when *P. aeruginosa* and *S. aureus* start as spatially separated single cells, we observed that *P. aeruginosa* uses the Pil-Chp chemoreceptor, PilJ, to respond from a distance by directionally moving toward *S. aureus* (42, 43). This attraction requires secretion of *S. aureus* peptides called phenol-soluble modulins (42, 44). However, it remains unknown how *P. aeruginosa* chemotaxis toward *S. aureus* influences *S. aureus* physiology and survival.

Here, we sought to understand the consequences of P. aeruginosa TFP-mediated attraction on S. aureus. We visualized P. aeruginosa and S. aureus interactions at the single-cell level over time using resonant scanning confocal microscopy and discovered that P. aeruginosa utilizes a combination of TFP-mediated motility and secreted antimicrobials to effectively outcompete S. aureus under these conditions. Particularly, we found that wild-type (WT) P. aeruginosa is attracted to, invades, and disrupts S. aureus colonies. Moreover, P. aeruginosa-secreted antimicrobials HQNO, pyoverdine, pyochelin, and LasA were necessary for negatively influencing S. aureus growth, but not for invasion and disruption of S. aureus colonies. Conversely, in the absence of TFP motility, P. aeruginosa cannot invade S. aureus colonies but rather grows around them, leading to an altered S. aureus colony architecture resulting in compact, thicker colonies with increased biomass compared with coculture with WT P. aeruginosa. In addition to these effects on S. aureus colony architecture, we also found that coculture with a TFP-deficient P. aeruginosa leads to altered physiology through the induction of an HQNO-mediated increase in S. aureus fermentation. Moreover, TFP motility was crucial for modulating the spatial arrangement and competitive dynamics between P. aeruginosa and S. aureus

September 2024 Volume 15 Issue 9 10.1128/mbio.00956-24 **2** 

in conditions that capture essential features of the CF airway environment. Overall, our findings highlight the importance of spatial organization in community-based behaviors and the need for a more thorough understanding of the interplay between polymicrobial communities in the context of infection.

#### **RESULTS**

#### TFP are necessary for P. aeruginosa invasion into S. aureus colonies

We previously reported that P. aeruginosa responds to S. aureus from a distance by using TFP to chemotax toward and surround S. aureus colonies (42), but how this behavior affects S. aureus physiology remained unclear. To test the consequences of P. aeruginosa chemotaxis on S. aureus, we first visualized P. aeruginosa interactions with S. aureus colonies in three dimensions by performing live resonant scanning confocal microscopy of S. aureus in mono- or coculture with P. aeruginosa WT or a TFP-deficient mutant (ΔpilA). Here, S. aureus and P. aeruginosa constitutively expressed sqfp (pseudocolored orange) and mCherry (pseudocolored cyan), respectively. Bacteria were inoculated between a cover slip and an agarose pad for visualization in the same visual field over time. Imaging was initiated with S. aureus and P. aeruginosa as single cells, positioned approximately 30 to 50 µm apart to provide sufficient time and distance for *P. aeruginosa* to respond to the presence of S. aureus. As previously demonstrated (42), at approximately 5 hours, we observed that WT P. aeruginosa responds to S. aureus by breaking into single cells and moving toward it with TFP motility, which eventually leads to P. aeruginosa surrounding, invading, and disrupting S. aureus cells from the colony (Fig. 1). This invasion is dependent on TFP motility, as P. aeruginosa ΔpilA exhibited significantly decreased invasion compared with WT (Fig. 1B). While the  $\Delta pilA$  mutant is amotile, it eventually grows against the S. aureus colony at later time points (Fig. 1A and C). These data suggest that TFP motility is not only necessary for P. aeruginosa chemotaxis toward S. aureus but also enables effective invasion of P. aeruginosa into S. aureus colonies.

### P. aeruginosa TFP motility-mediated invasion influences S. aureus growth and architecture

To investigate how P. aeruginosa invasion affects S. aureus colony physiology, we imaged S. aureus in mono- or coculture with WT or  $\Delta pilA$  P. aeruginosa following ~24 hours of incubation. At later time points, visualizing P. aeruginosa becomes challenging due to reduced fluorescence from decreased mCherry production and photobleaching. Nevertheless, phase contrast microscopy confirmed that P. aeruginosa cells surround S. aureus colonies after ~24 hours (Fig. S1).

We found that in coculture with WT P. aeruginosa, S. aureus forms smaller colonies than in monoculture by measuring the area at the base of the S. aureus colony (Fig. 2A and B). Moreover, P. aeruginosa TFP motility-mediated invasion resulted in S. aureus colony edges exhibiting reduced fluorescence, likely caused by dispersed, lysed cells, or a combination thereof (Fig. 2A). In the presence of  $\Delta pilA$ , the area of S. aureus colonies was comparable to that in the presence of WT P. aeruginosa (Fig. 2B). However, despite similar growth area, S. aureus colonies exhibited less dispersal at the colony edges in coculture with  $\Delta pilA$ , possibly due to loss of P. aeruginosa invasion (Fig. 2A; top and middle rows). Additionally, S. aureus colonies appeared thicker and denser than in coculture with WT P. aeruginosa, likely due to reduced cell dispersal.

To further investigate this, we visualized and quantified *S. aureus* colony architecture in more detail. Since thickness and density were more distinct on the colony edges, images were acquired with higher magnification and spatial resolution using galvanometric point-scanning confocal microscopy at the end time point (Fig. 2A; middle row). We then measured the height at the edge of *S. aureus* colonies at 15  $\mu$ m from the edge using the Z-plane (Fig. 2A, bottom row, and Fig. 2C). As expected, the height at the colony edge was significantly higher in coculture with  $\Delta pilA$  than in mono- or coculture with WT *P. aeruginosa* (Fig. 2C). To quantitatively analyze colony density, we measured

September 2024 Volume 15 Issue 9

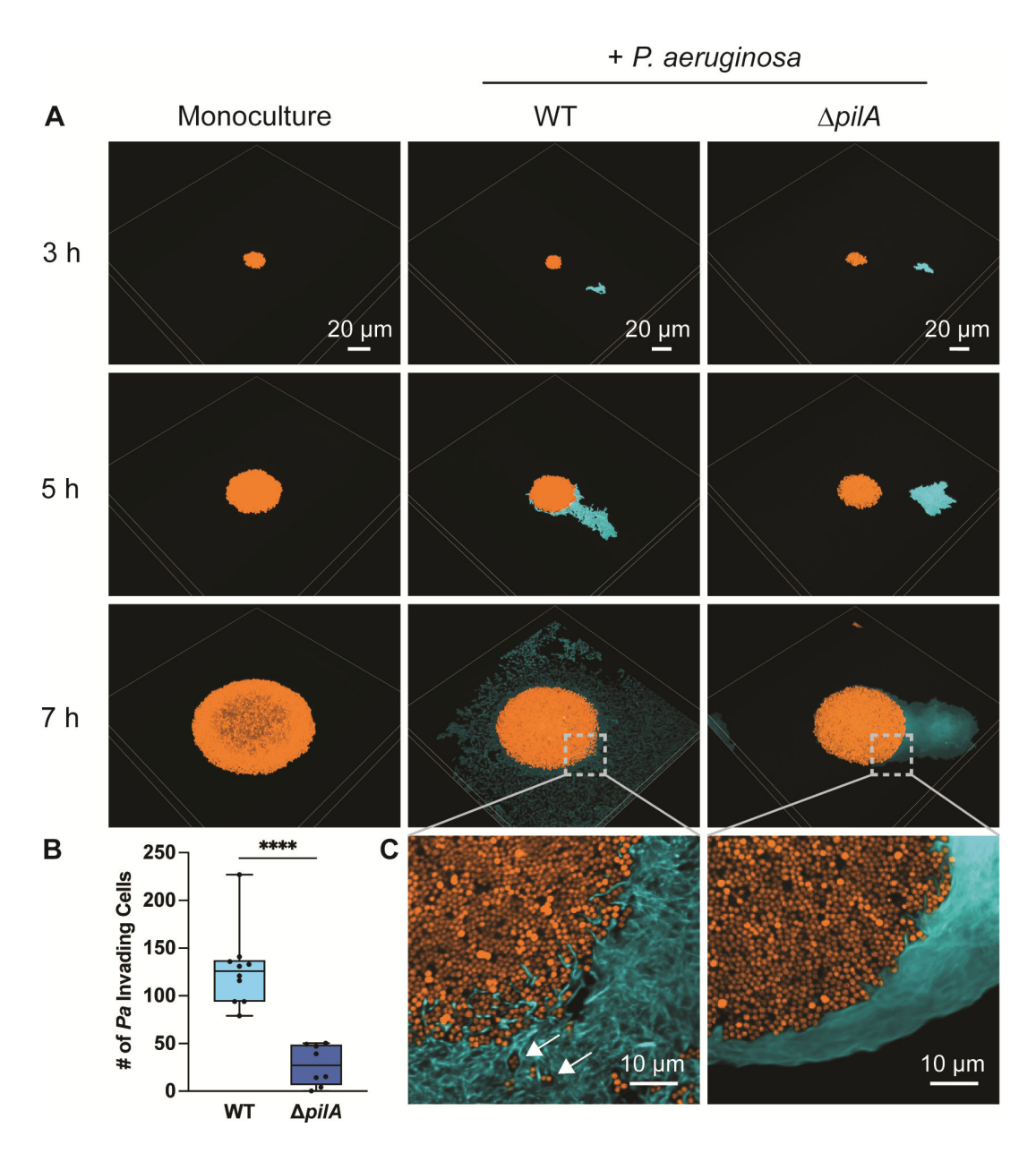


FIG 1 Type IV pili are necessary for *P. aeruginosa* invasion into *S. aureus* colonies. Resonant scanning confocal live imaging of *S. aureus* and *P. aeruginosa*. (A) Representative micrographs of WT *S. aureus* (pseudocolored orange) in monoculture or in coculture with *P. aeruginosa* (pseudocolored cyan; WT or TFP-deficient mutant  $\Delta pilA$ ). (B) Quantification of *P. aeruginosa* single-cell invasion into *S. aureus* colonies  $t \sim 7$  hours in mono- or coculture with *P. aeruginosa* (WT or  $\Delta pilA$ ). At least four biological replicates with two technical replicates each were analyzed. Each data point represents one technical replicate. Statistical significance was determined by a Mann-Whitney *U*-test. \*\*\*\*P < 0.0001. (C) Zoomed micrograph of *S. aureus* colony edge in coculture with *P. aeruginosa* (WT or  $\Delta pilA$ ). White arrows indicate dispersed *S. aureus* cells. *S. aureus*: pCM29 P<sub>SarAP1-safp</sub>; *P. aeruginosa*: chromosomal P<sub>A1/04/03-mCherry</sub>.

both cell packing and colony surface roughness using the microscopy image analysis software BiofilmQ (45). These parameters quantify density by measuring the amount of surface or volume within a specified area. In BiofilmQ, *S. aureus* colony edges were separated from the background by segmentation onto a 3D grid, with each cubic grid unit measuring 0.72  $\mu$ m per side. Neighborhood surface roughness and cell packing were then calculated by determining the biovolume fraction and surface height variance of *S. aureus* for each grid cube within 4 and 6  $\mu$ m, respectively. Representative heatmaps in Fig. 2D and E provide a two-dimensional visualization of the quantified data in Fig. 2F through H, using color coding to represent local surface roughness and cell packing. *S. aureus* colonies in monoculture show low surface roughness and uniform cell packing

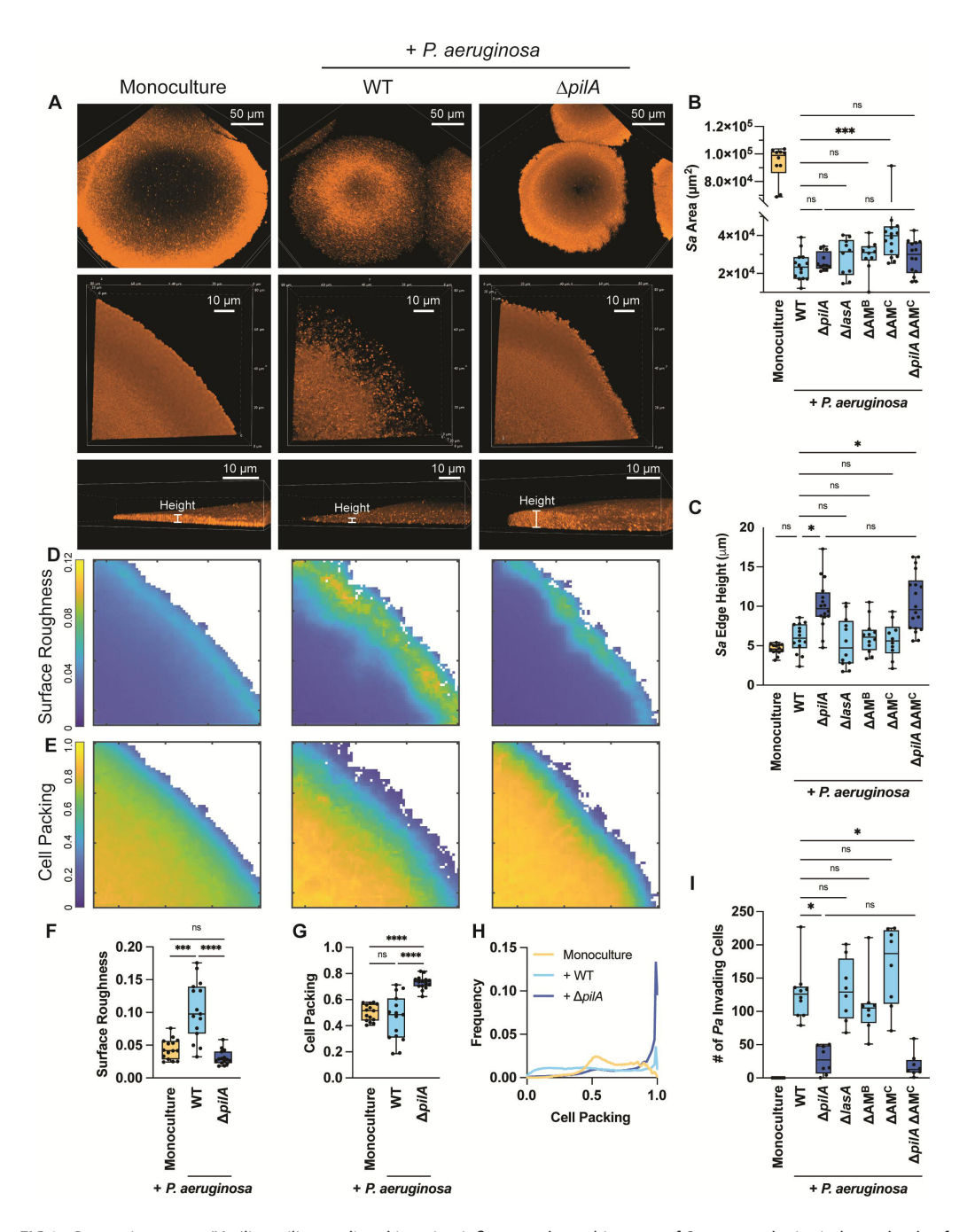


FIG 2 *P. aeruginosa* type IV pili motility-mediated invasion influences the architecture of *S. aureus* colonies independently of *P. aeruginosa*-secreted antimicrobials. Analysis of *S. aureus* colony edge disruption and thickness. (A) Representative resonant scanning confocal micrographs of the whole colony (top row) or Galvano scanner colony edge micrographs of WT *S. aureus* (orange) in monoculture or coculture with *P. aeruginosa* (not shown; WT or Δ*pilA*) at  $t \sim 24$  hours shown from the top (middle row) of the colony or the side (bottom row). The micrographs in A (bottom row) show the colonies on the Z-plane and demonstrate how the height was quantified. Quantification of *S. aureus* whole colony area at  $t \sim 24$  hours (B) or height at the edge of *S. aureus* (*Sa*) colony (μm) at  $t \sim 24$  hours (C) in monoculture or coculture with *P. aeruginosa* (WT, Δ*pilA*, Δ*lasA*, ΔΔM<sup>B</sup> [bacteriostatic antimicrobials; HQNO, pyoverdine, and pyochelin, ΔAM<sup>C</sup> [complete antimicrobials; HQNO, pyoverdine, pyochelin, and LasA], or Δ*pilA* ΔAM<sup>C</sup>). (D–G) Representative BiofilmQ heatmaps (D and E) and quantification (F and G) of local surface roughness and cell packing analysis at *S. aureus* colony edge in mono- or coculture with *P. aeruginosa* (WT or Δ*pilA*). Each data point represents the average of two technical replicates within one biological replicate. Statistical significance was determined by a Mann-Whitney *U*-test with an *ad hoc* Bonferroni correction for multiple comparisons. (H) Cell packing distribution within *S. aureus* colony edge in the abovementioned conditions. A Kolmogorov-Smirnov cumulative distribution (Continued on next page)

#### FIG 2 (Continued)

test was performed, and all three conditions were significantly different (\*\*\*\*P < 0.0001) from one another. A total of 15 biological replicates with two technical replicates each were analyzed in panels F–H. (I) The number of invading *P. aeruginosa* (*Pa*) single cells inside *S. aureus* was quantified at  $t \sim 7$  hours in mono- or coculture with the *P. aeruginosa* strains described above. At least four biological replicates with two technical replicates each were analyzed per condition in panels B, C, and I. Each data point represents one technical replicate. Statistical significance in panels B, C, and I was determined by Kruskal-Wallis followed by Dunn's multiple comparisons test. n.s., not significant; \*P < 0.001, \*\*\*\*P < 0.001, and \*\*\*\*\*P < 0.0001.

(Fig. 2D and E [first column] and Fig. 2F and G). Conversely, when WT P. aeruginosa is present, S. aureus edges exhibit significantly increased surface roughness and slightly decreased cell packing (Fig. 2D and E [middle column] and Fig. 2F and G), which suggests reduced colony density is caused by WT P. aeruginosa. When cocultured with ΔpilA (i.e., lacking invasion and colony disruption), S. aureus colonies portrayed significantly reduced colony surface roughness and increased cell packing compared with WT P. aeruginosa coculture (Fig. 2D and E [last column] and Fig. 2F and G). While the colony cell roughness was not different between S. aureus coculture with ΔpilA and monoculture, the mean colony cell packing was significantly increased (Fig. 2F and G). Additionally, we analyzed the cell packing distribution within S. aureus colony edges and found all three conditions to be statistically different (Fig. 2H). The majority of the monoculture colony edge population was distributed between 0.5 and 1.0, with almost no low-density areas. In S. aureus coculture with  $\Delta pilA$ , the large peak at 1.0 indicates that the majority of cells within these edges are highly packed. On the other hand, in the presence of WT P. aeruginosa, the cell packing is more evenly distributed with an increased proportion of the population at low-density values compared with monoculture or coculture with ΔpilA. However, there is also an increased proportion of the population at high-density values portrayed as a small peak at 1.0. This peak may be attributed to the colony edge height being slightly higher than monoculture S. aureus as reported in Fig. 2C, leading to higher cell packing as this calculation considers the three-dimensional space.

Thus, while the base area of the colony is similar in the presence of WT or  $\Delta pilA$ , the colonies are more densely packed when *P. aeruginosa* lacks TFP. Altogether, these observations reveal the crucial role of *P. aeruginosa* TFP motility in altering *S. aureus* architecture. Without TFP motility, *P. aeruginosa* does not invade or disrupt *S. aureus* colonies; instead, it grows alongside them, resulting in increased compaction and altered *S. aureus* colony structure.

# *P. aeruginosa* secretes antimicrobials that affect *S. aureus* growth but do not influence *S. aureus* colony architecture

Next, we wondered how invasion changes *S. aureus* colony architecture and enhances competition. One hypothesis is that invasion increases the local concentration of *P. aeruginosa* antimicrobials within *S. aureus* colonies. Additionally, these anti-staphylococcal factors could aid *P. aeruginosa* invasion. If the former is correct, *S. aureus* colonies grown in the presence of the *P. aeruginosa* Δ*pilA* would be protected from *P. aeruginosa* antimicrobials. *P. aeruginosa* secretes many factors known to inhibit or lyse *S. aureus*, including HQNO, a respiratory toxin that inhibits the *S. aureus* electron transport chain (30, 36), the siderophores pyoverdine and pyochelin, which aid in iron scavenging (29, 32), and an anti-staphylococcal protease, staphylolysin or LasA, which lyses *S. aureus* by cleaving the peptidoglycan pentaglycine cross-links (31).

Since  $\Delta pilA$  had reduced invasion and disruption of *S. aureus* exterior structure compared with WT, we first determined if this difference is due to variations in levels of secreted antimicrobials between the *P. aeruginosa* strains and tested whether  $\Delta pilA$  produces similar levels of exoproducts as WT. The cell-free supernatant from  $\Delta pilA$  or WT *P. aeruginosa* was added to *S. aureus* to examine its growth and lysis over time. No differences were observed in either *S. aureus* lysis or growth rate when exposed to supernatant from WT or  $\Delta pilA$  *P. aeruginosa*, confirming that each produces similar levels

September 2024 Volume 15 Issue 9 10.1128/mbio.00956-24 **6** 

of antimicrobials (Fig. S2). Here, supernatant from *P. aeruginosa ΔlasA* served as a control to confirm that staphylolysin is the main driver of *S. aureus* lysis.

To test the hypothesis that *P. aeruginosa* invasion enhances competition by increasing diffusion and local antimicrobial concentration within S. aureus colonies, we next examined S. aureus colony growth dynamics in the presence of P. aeruginosa strains lacking genes encoding antimicrobials. These include a staphylolysin mutant ( $\Delta lasA$ ), a strain without both HQNO and siderophores (ΔpqsL ΔpvdA ΔpchE), referred to as " $\Delta$ AM<sup>B</sup>" (antimicrobials <sup>Bacteriostatic</sup>), and a mutant with all four antimicrobials deleted ( $\Delta$ pqsL  $\Delta pvdA$   $\Delta pchE$   $\Delta lasA$ ) which we call " $\Delta AM^{C}$ " ( $AM^{Complete}$ ) in Fig. 2B, C and I. The interactions between S. aureus and these antimicrobial-deficient strains were assessed by live imaging as described for Fig. 1, and *P. aeruginosa* invasion and *S. aureus* colony height (as a proxy for biomass) were quantified. No detectable differences were observed between coculture with WT P. aeruginosa and the antimicrobial mutants for either the S. aureus colony edge height (Fig. 2C) or the number of invading cells (Fig. 2I), which suggests that these antimicrobials do not play a role in P. aeruginosa invasion or increased S. aureus colony height observed in coculture with  $\Delta pilA$ . Yet, it is known that these antimicrobials can impact *S. aureus* growth *in vitro* (11, 13, 15, 16, 35, 37, 38, 46). Therefore, we measured S. aureus colony base area to examine antimicrobial influence on growth under these conditions. The S. aureus colony area did not significantly increase when cocultured with  $\Delta AM^B$  or  $\Delta lasA$ , compared with the WT (Fig. 2B). However, colony area did increase upon deletion of all four antimicrobials ( $\Delta AM^{C}$ ), which suggests that while these antimicrobials do not influence S. aureus colony architecture, their combinatorial effect alters S. aureus growth and colony area.

To determine if *S. aureus* colony edge height and *P. aeruginosa* invasion are driven by motility alone or a combined effect of motility and antimicrobials, we deleted *pilA* in the  $\Delta AM^{C}$  mutant, generating  $\Delta pqsL$   $\Delta pvdA$   $\Delta pchE$   $\Delta lasA$   $\Delta pilA$  ( $\Delta pilA$   $\Delta AM^{C}$ ). *S. aureus* colony height and invasion of *P. aeruginosa*  $\Delta pilA$   $\Delta AM^{C}$  phenocopied  $\Delta pilA$  (Fig. 2C and I), suggesting that TFP motility plays a prominent role in driving these phenotypes. Furthermore, when comparing the effect of  $\Delta pilA$  on the WT background to the  $\Delta AM^{C}$  background, significant antimicrobial influence on the colony area is only observed when TFP are functional, supporting that motility may enhance antimicrobial action against *S. aureus* under these conditions (Fig. 2B).

Overall, these data suggest that thicker and denser *S. aureus* colony architecture is exclusively mediated by the absence of *P. aeruginosa* TFP-mediated colony invasion and that the main *P. aeruginosa* anti-staphylococcal factors do not substantially influence this observation. Furthermore, *P. aeruginosa* TFP motility may enhance antimicrobial access into the colony to fully affect *S. aureus* growth, revealing the important role *P. aeruginosa* motility plays in antagonistic interactions against *S. aureus*.

#### Increased cell packing enhances HQNO-mediated S. aureus fermentation

Although *P. aeruginosa* antimicrobials did not influence *S. aureus* structure, we next explored how colony morphology differences affect *S. aureus* physiological response to HQNO by utilizing a fluorescent reporter system. HQNO poisons the *S. aureus* respiratory chain, forcing a shift to fermentative metabolism (11); therefore, *S. aureus* fermentation can be used as a proxy for HQNO activity. A fluorescent transcriptional fusion to the promoter of the lactate dehydrogenase gene ( $P_{Idh1-sgfp}$ ) was used to measure fermentation (47). If HQNO penetrates densely packed colonies, we expect to see increased fluorescence compared with coculture with *P. aeruginosa* lacking HQNO production. To test this prediction, we live imaged *S. aureus* in mono- or coculture with *P. aeruginosa* and quantified the mean fluorescence intensity (MFI) per *S. aureus* colony over 18 hours (Fig. 3). *S. aureus*  $P_{Idh1-sgfp}$  fluorescence began to increase at approximately 12 hours in coculture with WT *P. aeruginosa* but did not increase in  $\Delta pqsL$  coculture, confirming prior reports that HQNO increases Idh expression (11). To test if fermentation increases in the absence of invasion,  $P_{Idh1-sgfp}$  expression was quantified in coculture with *P. aeruginosa*  $\Delta pilA$ . Notably, we observed a sharp increase in fermentation of densely packed colonies

September 2024 Volume 15 Issue 9 10.1128/mbio.00956-24 **7** 

produced by coculture with ΔpilA (shown in Fig. 3A; quantified in Fig. 3B and C). One interpretation of these data is that HQNO concentrates within densely packed colonies, inducing a more dramatic change in S. aureus physiology. Additionally, since ΔpilA cells grow around and against S. aureus, it is possible that the striking increase in S. aureus fermentation is due to more HQNO-producing cells surrounding S. aureus colonies, although precisely quantifying the cell number under these conditions is technically challenging. Alternatively, the increased P<sub>Idh1-sqfp</sub> signal may result from increased cell density, independent of HQNO, potentially due to oxygen restriction within the colony. To differentiate these possibilities, fermentation was measured in the presence of a  $\Delta pqsL$ ΔpilA mutant. As seen with motile ΔpqsL, the double mutant does not induce S. aureus fermentation over time (Fig. 3B), suggesting HQNO mediates this increased fermentation. Importantly, the phenotypes of both  $\Delta pilA$  and  $\Delta pqsL$  mutants were genetically complemented by expressing their respective genes in cis ( $\Delta pilA$ ) or trans ( $\Delta pqsL$ ) under control of an inducible promoter (Fig. S3). These findings show that HQNO likely diffuses into S. aureus colonies independently of P. aeruginosa invasion and plays a crucial role in mediating interspecies interactions by pushing *S. aureus* toward fermentation.

### *P. aeruginosa* TFP motility is necessary for competition against *S. aureus* in conditions that mimic CF lung secretions

So far, we see a role for TFP motility in competition against *S. aureus* under conditions that constrain cells to the surface. While useful for high spatial and temporal resolution, this approach does not accurately reflect other attributes of the CF airway infection environment. Thus, we sought to determine whether TFP motility drives interactions when cocultured under conditions that mimic CF lung secretions by using artificial sputum media (ASM) (5), a modified version of SCFM2 (48). ASM captures some of the essential features of the CF environment, like constraints on movement and diffusion, that shaken liquid culture methods do not, and similar recipes have been shown to recapitulate approximately 86% of *P. aeruginosa* gene expression in human-expectorated CF sputum, outperforming both laboratory media and the acute mouse pneumonia model of infection (49, 50).

S. aureus and P. aeruginosa (WT or  $\Delta pilA$ ) at a 1:1 ratio were grown statically for 22 hours and imaged with resonant scanning confocal microscopy to visualize their spatial organization. The end time point was plated for colony-forming units to assess bacterial viability. In the presence of WT motile P. aeruginosa, S. aureus was suppressed relative to its monoculture condition: very few S. aureus cells could be observed or counted (Fig. 4A and B), compared with approximately 108 CFUs/well recovered in S. aureus monoculture. However, when S. aureus was grown with P. aeruginosa ΔpilA, a 100– 10,000-fold increase in S. aureus cells was recovered in comparison to coculture with WT P. aeruginosa (Fig. 4B). Overall, this suggests that TFP motility is necessary for effective competition with S. aureus in ASM. TFP are also necessary for P. aeruginosa biofilm formation and attachment to surfaces (51–53). However, we observed that P. aeruginosa biofilm formation and spatial organization were similar in appearance between WT and ΔpilA in coculture with S. aureus in ASM (Fig. 4A). While the CFUs/well recovered for ΔpilA were significantly lower than WT P. aeruginosa in mono- or coculture with S. aureus (Fig. 4C), the difference is modest (~95% of WT) and thus not expected to account for the increase in S. aureus survival. Next, we tested if the mere presence of TFP has a role in competition or if TFP motility is required. To differentiate between these two outcomes, a hyperpiliated, non-twitching *P. aeruginosa* mutant (Δ*pilT*) was cocultured with *S. aureus*. This mutant lacks the main retraction ATPase of the TFP machinery, PilT, and is well documented to ineffectively retract extended pili (54). S. aureus survival in the presence of  $\Delta pilT$  phenocopied  $\Delta pilA$  (Fig. 4A and B), suggesting that functional TFP are necessary for competitive interactions with S. aureus in ASM. Collectively, these data demonstrate that under CF-relevant conditions, P. aeruginosa TFP motility aids in interspecies competition.

September 2024 Volume 15 Issue 9

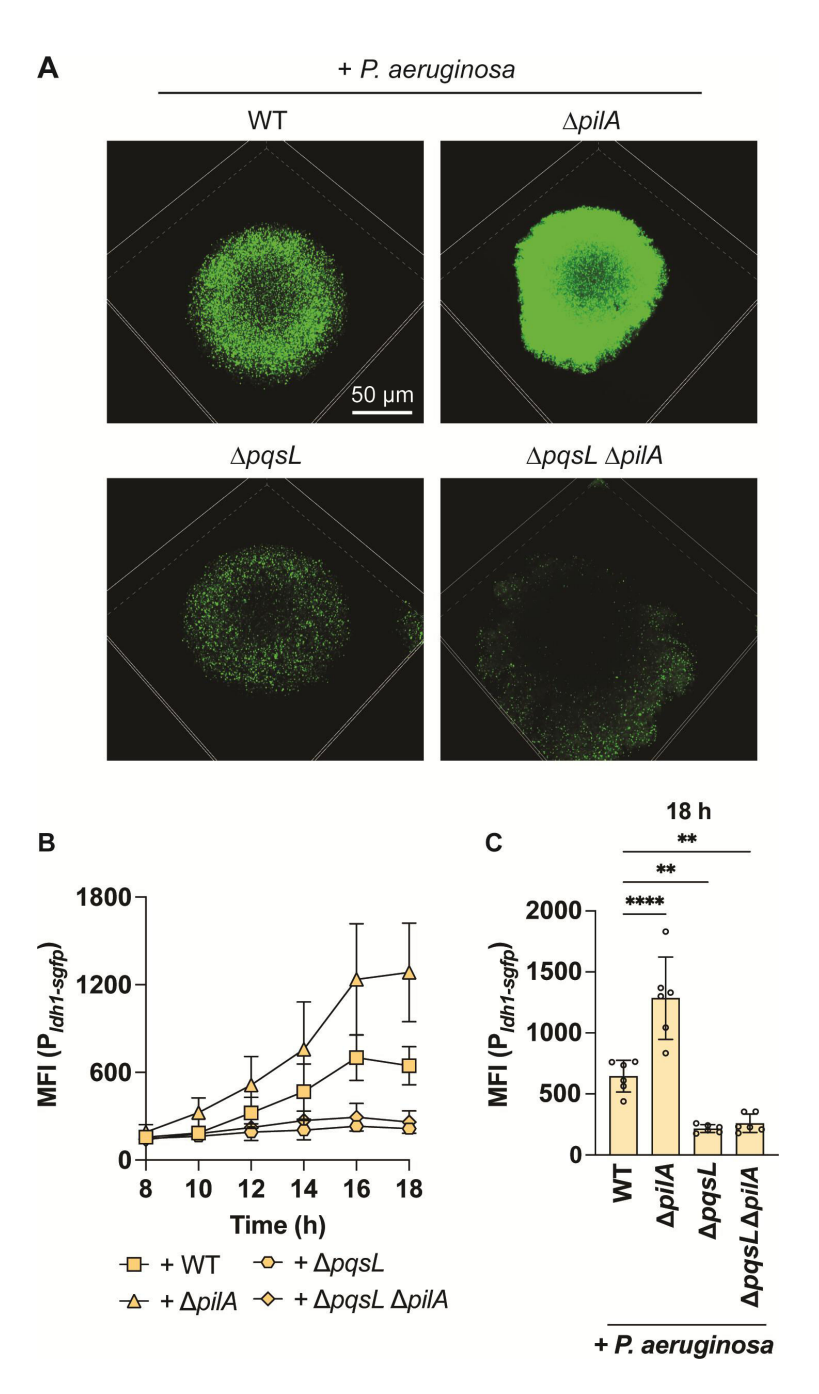


FIG 3 Increased *S. aureus* cell packing enhances HQNO-mediated *S. aureus* fermentation. *S. aureus* lactic acid fermentation ( $P_{Idh1-sgfp}$ ) was measured in the presence of the indicated *P. aeruginosa* strains. (A) Representative resonant scanning confocal micrographs of *S. aureus* fermentation in coculture with *P. aeruginosa* (WT,  $\Delta pilA$ ,  $\Delta pqsL$ , or  $\Delta pqsL$   $\Delta pilA$ ) t=18 hours, *S. aureus* channel only. (B) MFI (fluorescence/colony volume) was quantified over time. (C) MFI at 18 hours. Data represent the mean and standard deviation from three biological replicates with two technical replicates per condition. Each data point represents one technical replicate. Statistical analyses were performed at 18 hours using one-way ANOVA followed by Dunnett's multiple comparisons test comparing each condition to +WT *P. aeruginosa*. \*\*P < 0.01 and \*\*\*\*P < 0.0001.

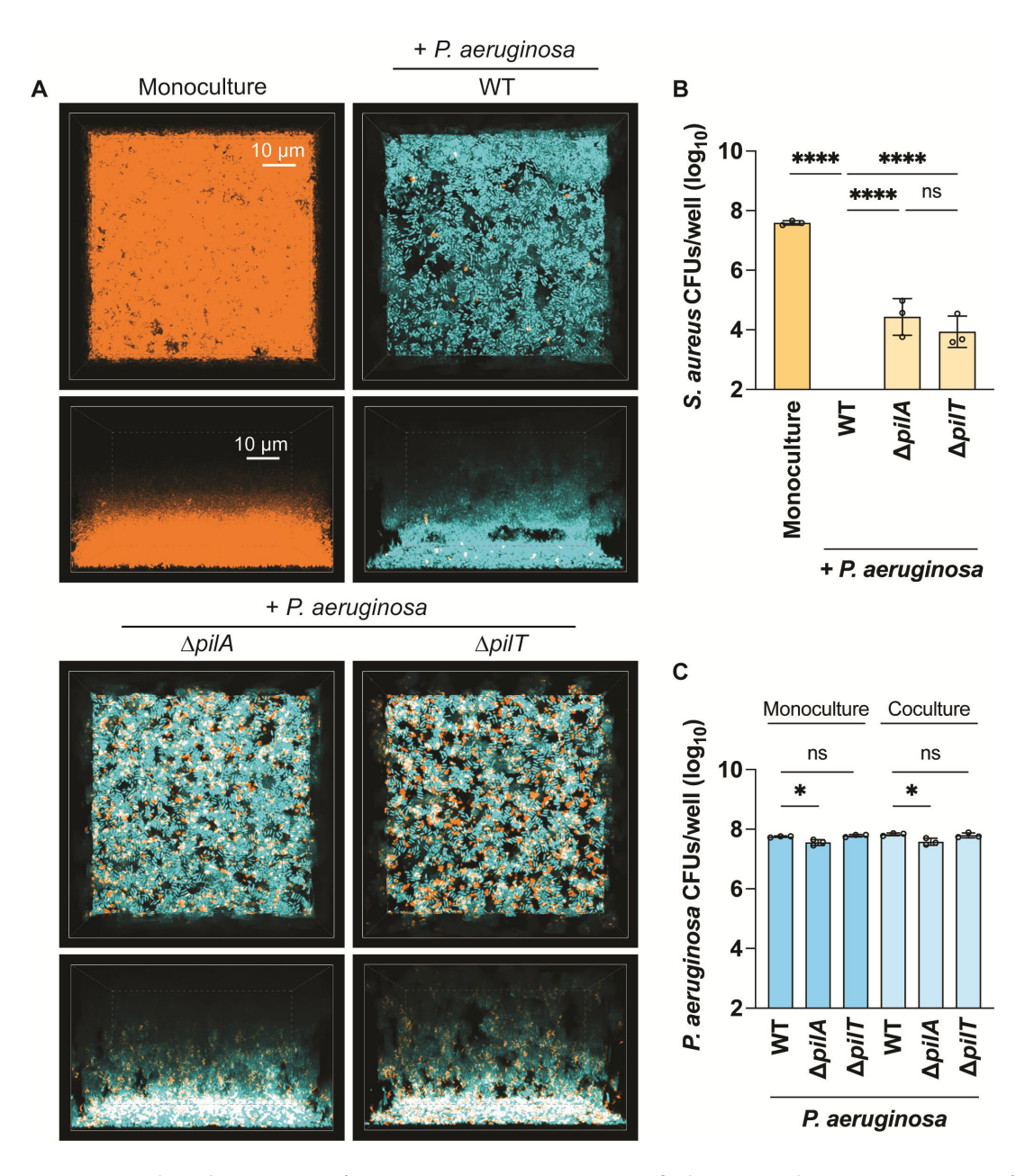


FIG 4 *P. aeruginosa* type IV pili motility is necessary for competition against *S. aureus* in artificial sputum media. Resonant scanning confocal imaging of *S. aureus* and *P. aeruginosa* under static conditions in artificial sputum media, with CFU quantification. (A) Representative images of resonant scanning confocal micrographs of WT *S. aureus* (pseudocolored orange) in monoculture or in coculture with *P. aeruginosa* (pseudocolored cyan; WT,  $\Delta pilA$ , or  $\Delta pilT$ )  $t \sim 22$  hours. White indicates areas of overlap between *S. aureus* and *P. aeruginosa* suggesting colocalization. *S. aureus* (B) or *P. aeruginosa* (C) CFU quantification in monoculture or in coculture with *P. aeruginosa* (WT,  $\Delta pilA$ , or  $\Delta pilT$ ) (B) or in mono- or coculture with *S. aureus* (C) at t = 24 hours. The CFUs/well in *Y*-axes are portrayed as  $\log_{10}$  transformed. Three biological replicates with one technical replicate each were analyzed, and the mean and standard deviation are shown. Each data point represents one biological replicate. Statistical significance was determined by one-way ANOVA followed by Dunnett's multiple comparisons test. n.s., not significant; \* $^{*}P < 0.05$  and \*\*\*\* $^{*}P < 0.0001$ .

## *P. aeruginosa* TFP motility is necessary for disruption and competition against pre-formed *S. aureus* biofilms

Next, we asked if *P. aeruginosa* TFP motility is necessary for competition against preformed (5 hours) *S. aureus* biofilms in ASM. *P. aeruginosa* WT,  $\Delta pilA$ , or  $\Delta pilT$  were added to *S. aureus* and allowed to grow for an additional 24 hours before imaging and plating for viability. Remarkably, we found that WT *P. aeruginosa* invades and disrupts pre-formed *S. aureus* biofilms, as depicted in Fig. 5A (Z plane) and Movie S1, where a layer of the

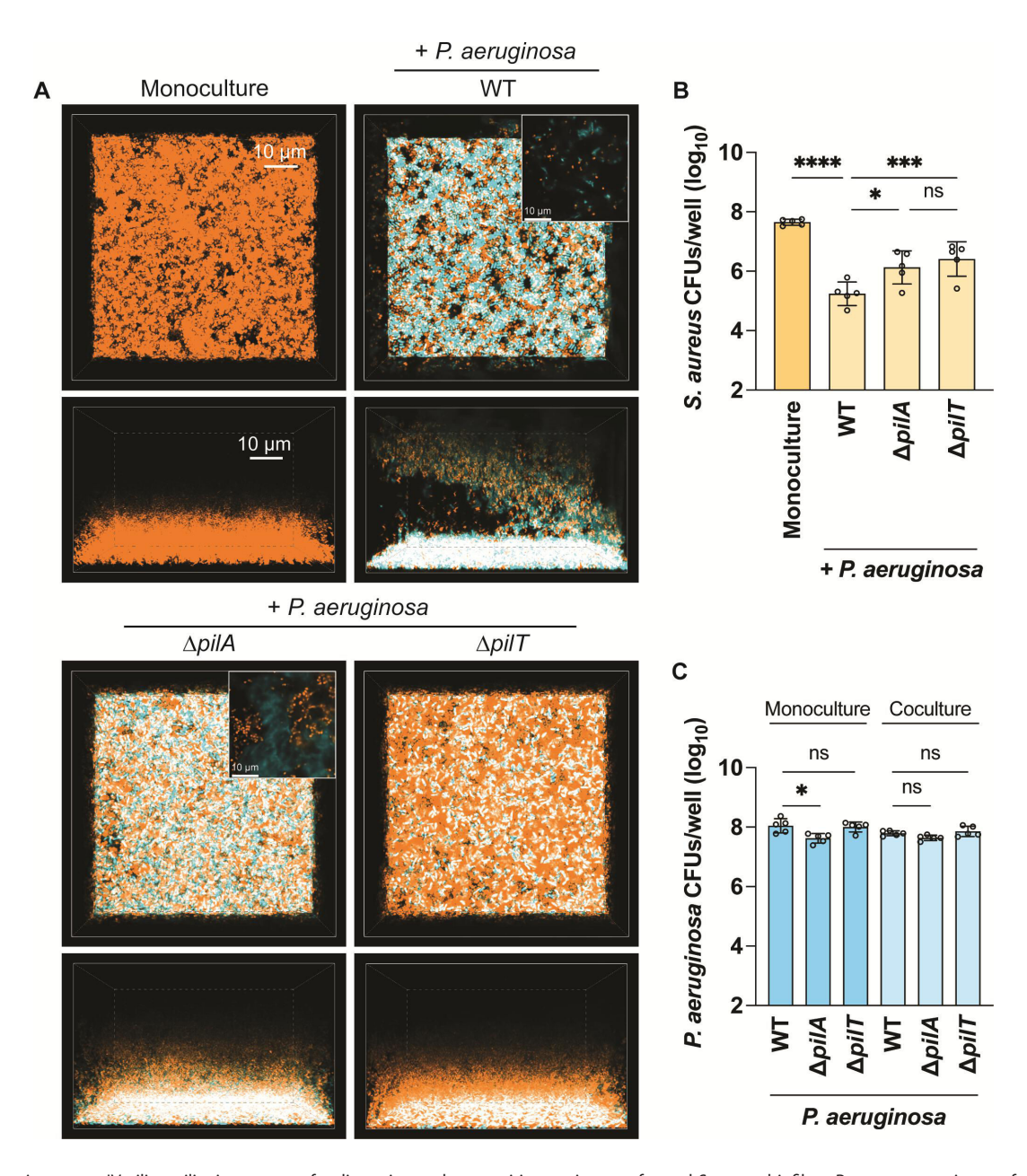


FIG 5 *P. aeruginosa* type IV pili motility is necessary for disruption and competition against pre-formed *S. aureus* biofilms. Resonant scanning confocal imaging of *S. aureus* and *P. aeruginosa* under static conditions in artificial sputum media, with CFU quantification at late time points. *P. aeruginosa* was added to *S. aureus* pre-formed biofilms at 5 hours. (A) Representative images of resonant scanning confocal micrographs of WT *S. aureus* (pseudocolored orange) in monoculture or in coculture with *P. aeruginosa* (pseudocolored cyan; WT,  $\Delta pilA$ , or  $\Delta pilT$ )  $t \sim 26$  hours. The insets show  $\sim 3 \times$  zoomed images at 30 µm from the base of the coverslip. White indicates areas of overlap between *S. aureus* and *P. aeruginosa* suggesting colocalization. *S. aureus* (B) or *P. aeruginosa* (C) CFU quantification in mono- or in coculture with *P. aeruginosa* (WT,  $\Delta pilA$ , or  $\Delta pilT$ ) (B) or in mono- or coculture with *S. aureus* (C) at  $t \sim 29$  hours. The CFUs/well in *Y*-axes are portrayed as log<sub>10</sub> transformed. Five biological replicates with one technical replicate each were analyzed, and the mean and standard deviation are shown. Statistical significance was determined by one-way ANOVA followed by Dunnett's multiple comparisons test. n.s., not significant; \* $^{*}P < 0.05$ , \*\* $^{**}P < 0.001$ , and \*\*\* $^{**}P < 0.0001$ .

S. aureus biofilm detaches from the surface and is blanketed by P. aeruginosa cells. Disruption was dependent on P. aeruginosa TFP motility, as WT P. aeruginosa disrupted S. aureus pre-formed biofilms significantly more than  $\Delta pilA$  or  $\Delta pilT$  (Fig. S4). Notably, S. aureus and P. aeruginosa  $\Delta pilA$  remained segregated into monoculture aggregates, while cells were well mixed during coculture with motile P. aeruginosa (Fig. 5A, inset). These observations were consistent with results under agarose pads. We also observed that a higher number of WT P. aeruginosa colonized the surface of the coverslip compared

with the  $\Delta pilA$  or  $\Delta pilT$  mutants in the presence of *S. aureus* (Fig. 5A; Fig. S4). These data suggest that TFP motility is necessary for *P. aeruginosa* cells to invade from the top of *S. aureus* biofilms and traverse through to access the coverslip, potentially disrupting and detaching the biofilms in the process. This results in a significant reduction in *S. aureus* viability (10–15-fold) when comparing *S. aureus* coculture with WT versus  $\Delta pilA$  or  $\Delta pilT$  (Fig. 5B). Importantly, no viability differences were observed between *P. aeruginosa* WT and  $\Delta pilT$  (Fig. 5C). While  $\Delta pilA$  shows a significant decrease in viability compared with WT, it is unlikely to have a biological influence on *S. aureus* growth (Fig. 5C). Altogether, these observations suggest that TFP motility enhances *P. aeruginosa* competitive fitness, allowing it to disrupt and potentially render *S. aureus* cells more vulnerable to *P. aeruginosa* antimicrobials.

#### **DISCUSSION**

Growing data support the hypothesis that spatial organization is crucial in shaping microbial communities and influencing community-based behaviors (4, 5, 39, 55–61). In this study, we found that *P. aeruginosa* motility plays a vital role in shaping the biogeography in *S. aureus* cocultures. By influencing spatial aggregation, *P. aeruginosa* TFP motility ultimately dictates *S. aureus* physiology and survival.

While *P. aeruginosa* antimicrobials have been well documented to influence *S. aureus* growth and survival (11–16), *P. aeruginosa* motility in interspecies competition has only begun to be explored. We recently reported that *P. aeruginosa* senses *S. aureus*-secreted PSM peptides from a distance by the PilJ chemoreceptor (43). Consequently, it employs TFP motility to chemotax toward *S. aureus* colonies or PSMs alone (42, 44). In addition to chemotaxis, *S. aureus* PSMs also trigger a "competition sensing" response whereby *P. aeruginosa* upregulates type VI secretion system and pyoverdine biosynthesis pathways (44). Similarly, *P. aeruginosa* has been reported to utilize TFP-mediated motility to perform "suicidal chemotaxis" toward antibiotics (62). The upregulation of these common interbacterial competition pathways supports a model where *P. aeruginosa* senses potential danger in the environment and responds with directional twitching, while simultaneously activating defense mechanisms to combat the "enemy". Additionally, it has been reported that *P. aeruginosa* upregulates antimicrobial production upon sensing *N*-acetylglucosamine alone or shed from Gram-positive bacteria (63).

Our single-cell level temporal analysis also revealed that P. aeruginosa TFP motility is necessary for invading and disrupting S. aureus colonies (Fig. 1). Interestingly, loss of invasion leads P. aeruginosa to grow adjacent to S. aureus colonies, potentially acting as a "wall" to prevent expansion of the S. aureus colonies, which become thicker and denser (Fig. 2). While P. aeruginosa anti-staphylococcal factors did not mediate invasion into S. aureus colonies, they did influence growth as S. aureus formed larger colonies in the absence of P. aeruginosa antimicrobials HQNO, pyoverdine, pyochelin, and staphylolysin (Fig. 2B), as expected based on prior reports (11, 13, 16). However, most studies have been performed with P. aeruginosa cell-free supernatant and not with live P. aeruginosa present. Imaging P. aeruginosa and S. aureus in coculture at the single-cell level has allowed us to visualize the importance of P. aeruginosa motility in their interactions and, therefore, start to build a model whereby TFP motility aids in competition by disrupting S. aureus single cells away from the colony, leaving them exposed and more vulnerable to P. aeruginosa-secreted factors (Fig. 6). Therefore, when P. aeruginosa cannot move, we hypothesize that S. aureus cells remain protected within the colony and resist infiltration of P. aeruginosa antimicrobials. Altogether, these findings provide additional support of how TFP motility can either enhance competition or foster coexistence with S. aureus.

Different *S. aureus* colony morphology is a consequence of limited invasion by *P. aeruginosa*  $\Delta pilA$ , compared with WT, and shows a striking change in physiology by increasing fermentation ( $P_{ldh1-sgfp}$ ) (Fig. 3). While we initially hypothesized that *S. aureus* cells remained protected from *P. aeruginosa* antimicrobials in the absence of invasion, these data suggest that HQNO can diffuse into *S. aureus* colonies and alter growth and physiology without *P. aeruginosa* TFP-mediated invasion. Nevertheless, deletion of

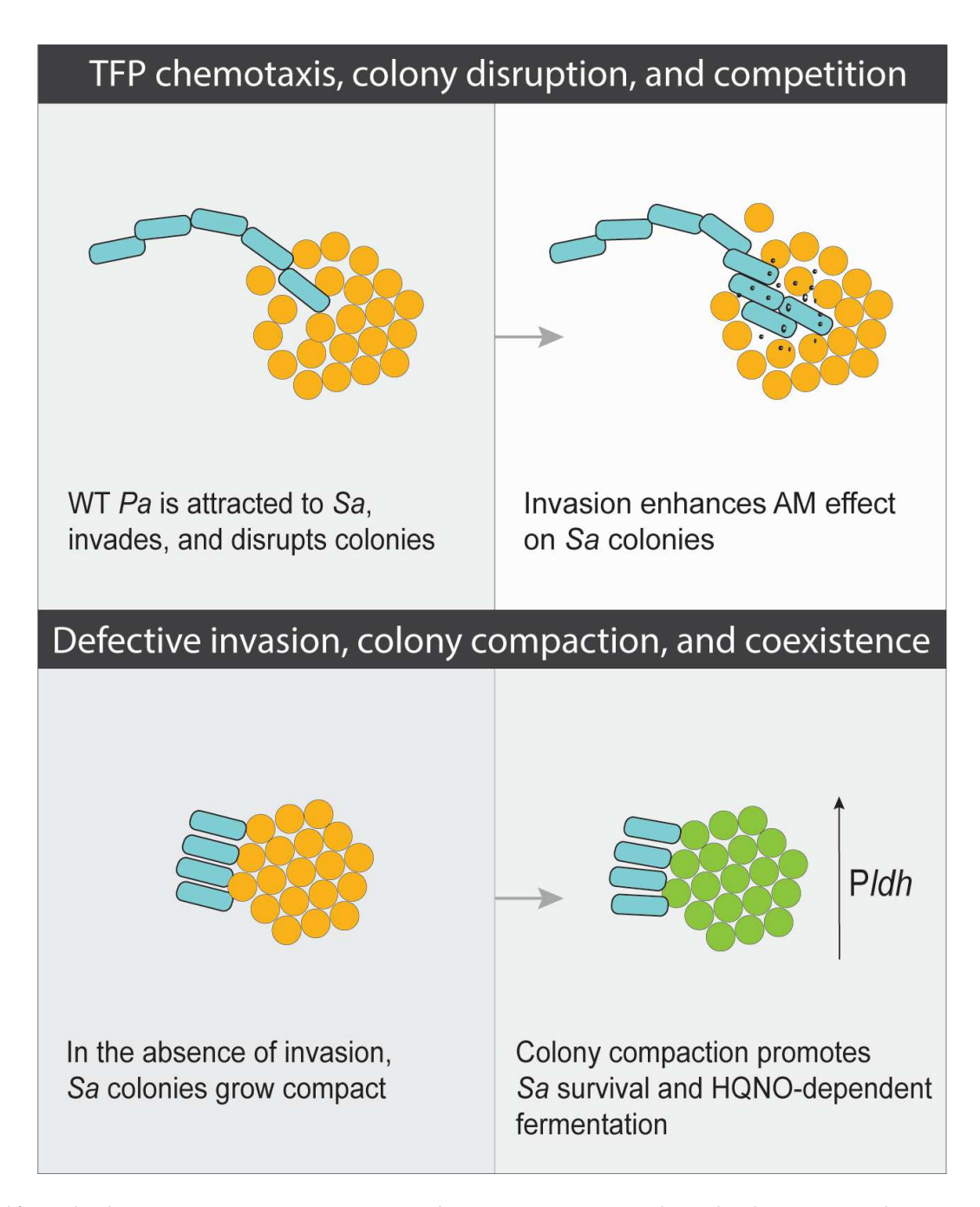


FIG 6 Model for motility-driven interspecies competition. We propose that *P. aeruginosa* (*Pa*) TFP motility-mediated attraction toward, invasion, and disruption of *S. aureus* (*Sa*) colonies promote the diffusion of antimicrobials (AM) to maximize interspecies competition. Lack of motility affects *S. aureus* spatial organization and physiology in a manner that promotes coexistence.

antimicrobial production in the  $\Delta pilA$  mutant background does not significantly improve *S. aureus* survival, as it does in the WT background. This observation supports the role of TFP-mediated invasion and disruption in allowing these antimicrobials to access *S. aureus* cells within the colonies for greater impact on its growth (Fig. 2B). Therefore, we hypothesize that without invasion and disruption, antimicrobials with higher molecular weight, such as staphylolysin (20 kDa), are precluded from freely diffusing into *S. aureus* colonies, while smaller compounds like HQNO (0.259 kDa) can diffuse and concentrate within *S. aureus*, eliciting physiological changes that could pose greater challenges for the effective treatment of infections.

Importantly, *P. aeruginosa* TFP motility's role in mediating interspecies competition and spatial aggregation was highlighted under conditions that mimic the nutritional and viscoelastic properties of CF airways. Of note, *P. aeruginosa* was capable of detaching preformed *S. aureus* biofilms and significantly reducing *S. aureus* viability in a motility-dependent manner when grown in ASM. These results emphasize the importance of motility in this CF-like polymicrobial environment.

The mucoid *P. aeruginosa* phenotype, a common adaptation that *P. aeruginosa* exhibits during CF infections, is associated with decreased competition against *S. aureus* due to the reduced production of anti-staphylococcal factors (46). Additional studies have demonstrated that another common adaptation of *P. aeruginosa* linked to chronic CF infections is reduced motility (64). Interestingly, *P. aeruginosa* mucoid and reduced twitching phenotypes have been identified as the best phenotypic predictors of future pulmonary exacerbations in children with CF (64). Our studies revealed that impairing twitching motility hinders *P. aeruginosa* competitiveness and promotes coexistence with *S. aureus* under CF-relevant conditions. This may be a contributing explanation for why *P. aeruginosa* and *S. aureus* are still found in high numbers in people with CF (18).

Extensive discussion surrounds whether *P. aeruginosa* and *S. aureus* encounter each other in CF lungs and if they compete or coexist (4, 39, 46, 55). CF airways are indeed a complex environment with multiple, distinct niches within; therefore, we predict that *P. aeruginosa* and *S. aureus* can coexist in some areas, while *P. aeruginosa* might outcompete *S. aureus* in others. They may be well mixed in some spaces and spatially segregated in others but still influence each other through the diffusion of secreted factors. As evidenced by both this study and others, it is clear that interspecies competition or coexistence can greatly depend on bacterial and host genotype and phenotype. Our *in vitro* data show how spatial organization can determine the outcome of microbe-microbe interactions and inform the potential interactions of these bacteria during infection. However, the CF airways are complex and involve other microorganisms and host factors that must be considered. Therefore, future experiments should explore these interactions *in vivo* and *ex vivo* to map the community biogeography and further elucidate interspecies dynamics.

Overall, our study reveals how *P. aeruginosa* TFP motility aids in the disruption of *S. aureus* colonies and biofilms, which potentiates the effect of *P. aeruginosa*-secreted anti-staphylococcal factors on *S. aureus* cells. Ultimately, *P. aeruginosa* motility plays a crucial and previously unexplored role in determining *S. aureus* outcome.

#### **MATERIALS AND METHODS**

For additional details on all the methods, see the supplemental materials and methods in Text S1.

#### **Bacterial strains and growth conditions**

See Text S1 for details on bacterial growth conditions. A list of strains used in this study can be found in Table S1.

#### Generation of *P. aeruginosa* deletion mutants

Markerless deletion mutants of genes in PA14 were constructed through homologous recombination as previously described (65).

#### Time-lapse microscopy

*P. aeruginosa* and *S. aureus* were cocultured under agarose pads as previously described (42) and live imaged with resonant scanning confocal microscopy.

#### S. aureus colony edge height and density measurements

*P. aeruginosa* and *S. aureus* were cocultured under agarose pads for ~24 hours and imaged with galvanometer scanning confocal microscopy. *S. aureus* colony edge height and density were analyzed in Nikon Elements and BiofilmQ (45), respectively.

#### S. aureus lactic acid fermentation (P<sub>Idh1-sqfp</sub>) quantification

*P. aeruginosa* and *S. aureus* were cocultured under agarose pads and live imaged with resonant scanning confocal microscopy. *S. aureus* lactic acid fermentation was quantified by measuring the mean fluorescence intensity ( $P_{Idh1-safp}$ ) of whole colonies over time.

#### Artificial sputum media assay

*P. aeruginosa* and *S. aureus* were cocultured in ASM for ~24 or 29 hours and imaged with resonant scanning confocal microscopy. ASM was prepared as previously described (5).

#### S. aureus lysis assay and growth curve with P. aeruginosa supernatant

*S. aureus* lysis in the presence of *P. aeruginosa* cell-free supernatant was assessed by modifying a previously published method (66). *S. aureus* growth with *P. aeruginosa* supernatant was assessed in a plate reader for 18 hours.

#### **ACKNOWLEDGMENTS**

We thank Dr. George O'Toole's lab and Dr. Timothy Yahr for generously providing bacterial strains and plasmids. We also thank Dr. Michael Gebhardt and members of the Limoli lab for their insightful feedback on the manuscript.

This work was supported by funding from the Cystic Fibrosis Foundation: CFF Postdoc-to-Faculty Transition Award LIMOL118F5 (D.H.L.), CFF RDP Junior Faculty Recruitment Award LIMOL119R3 (D.H.L.), funding from the National Institutes of Health: Maximizing Investigators' Research Award R35GM142760 (D.H.L.), 1R35GM151158-01 (C.D.N.), the Molecular & Cellular Biology of the Lung Training Grant 5T32HL007638-34 (A.S.-P.), and the T32 Training Grant Al007519 (J.B.W.). Additional support was provided by the John H. Copenhaver Jr. Fellowship (J.B.W.), the GAANN Fellowship (J.B.W.), the Human Frontier Science Program RGY0077/2020 (C.D.N.), the Simons Foundation 826672 (C.D.N.), and by the National Science Foundation IOS grant 2017879 (C.D.N.).

Funders had no role in the study design, data collection and interpretation, or the decision to submit the work for publication.

#### **AUTHOR AFFILIATIONS**

<sup>1</sup>Department of Microbiology and Immunology, Carver College of Medicine, University of Iowa, Iowa City, Iowa, USA

<sup>2</sup>Department of Biological Sciences, Dartmouth College, Hanover, New Hampshire, USA

#### **AUTHOR ORCIDs**

Andrea Sánchez-Peña http://orcid.org/0000-0002-4843-3652

James B. Winans http://orcid.org/0009-0000-2205-290X

Carey D. Nadell http://orcid.org/0000-0003-1751-4895

Dominique H. Limoli http://orcid.org/0000-0002-4130-337X

#### **FUNDING**

Funder	Grant(s)	Author(s)
Cystic Fibrosis Foundation (CFF)	LIMOLI18F5,LIMOLI19R3	B Dominique H. Limoli

September 2024 Volume 15 Issue 9 10.1128/mbio.00956-24**15** 

<sup>&</sup>lt;sup>3</sup>Department of Biology, Indiana University, Bloomington, Indiana, USA

Funder	Grant(s)	Author(s)
HHS   National Institutes of Health (NIH)	R35GM142760	Dominique H. Limoli
John H. Copenhaver Jr. Fellowship		James B. Winans
GAANN Fellowship		James B. Winans
Human Frontier Science Program (HFSP)	RGY0077/2020	Carey D. Nadell
National Science Foundation (NSF)	2017879	Carey D. Nadell
HHS   National Institutes of Health (NIH)	1R35GM151158-01	Carey D. Nadell
HHS   National Institutes of Health (NIH)	5T32HL007638-34	Andrea Sánchez-Peña
HHS   National Institutes of Health (NIH)	Al007519	James B. Winans

#### **ADDITIONAL FILES**

The following material is available online.

#### Supplemental Material

Text S1 (mBio00956-24-s0001.pdf). Supplemental materials and methods.

**Figure S1 (mBio00956-24-s0002.tif).** *P. aeruginosa* cells surround *S. aureus* colonies at the end time point.

**Figure S2** (mBio00956-24-s0003.tif). Exoproducts from  $\Delta pilA$  lyse and inhibit *S. aureus* to the same levels as WT *P. aeruginosa* factors.

Figure S3 (mBio00956-24-s0004.tif). Genetic complementation of pqsL or pilA.

**Figure S4 (mBio00956-24-s0005.tif).** *P. aeruginosa* type IV pilus motility is necessary for disrupting pre-formed *S. aureus* biofilms.

Supplemental Figures (mBio00956-24-s0006.pdf). Supplemental figures.

Supplemental Tables (mBio00956-24-s0007.pdf). Tables S1 to S3.

**Movie S1 (mBio00956-24-s0008.mov).** WT *P. aeruginosa* (cyan) disrupts *S. aureus* (orange) biofilms in ASM. Movie is at 29 hours.

#### **REFERENCES**

- Strassmann JE, Gilbert OM, Queller DC. 2011. Kin discrimination and cooperation in microbes. Annu Rev Microbiol 65:349–367. https://doi. org/10.1146/annurev.micro.112408.134109
- Filkins LM, O'Toole GA. 2015. Cystic fibrosis lung infections: polymicrobial, complex, and hard to treat. PLoS Pathog 11:e1005258. https://doi. org/10.1371/journal.ppat.1005258
- Little W, Black C, Smith AC. 2021. Clinical implications of polymicrobial synergism effects on antimicrobial susceptibility. Pathogens 10:144. https://doi.org/10.3390/pathogens10020144
- Limoli DH, Hoffman LR. 2019. Help, hinder, hide and harm: what can we learn from the interactions between *Pseudomonas aeruginosa* and *Staphylococcus aureus* during respiratory infections? Thorax 74:684–692. https://doi.org/10.1136/thoraxjnl-2018-212616
- Jean-Pierre F, Hampton TH, Schultz D, Hogan DA, Groleau M-C, Déziel E, O'Toole GA. 2023. Community composition shapes microbial-specific phenotypes in a cystic fibrosis polymicrobial model system. Elife 12:e81604. https://doi.org/10.7554/eLife.81604
- Jean-Pierre F, Vyas A, Hampton TH, Henson MA, O'Toole GA. 2021. One versus many: polymicrobial communities and the cystic fibrosis airway. mBio 12:e00006-21. https://doi.org/10.1128/mBio.00006-21
- McCully L.M, Bitzer AS, Seaton SC, Smith LM, Silby MW. 2019. Interspecies social spreading: interaction between two sessile soil bacteria leads to emergence of surface motility. mSphere 4:e00696-18. https://doi.org/10.1128/mSphere.00696-18
- Lozano GL, Bravo JI, Garavito Diago MF, Park HB, Hurley A, Peterson SB, Stabb EV, Crawford JM, Broderick NA, Handelsman J. 2019. Introducing THOR, a model microbiome for genetic dissection of community behavior. mBio 10:e02846-18. https://doi.org/10.1128/mBio.02846-18

- Hurley A, Chevrette MG, Rosario-Meléndez N, Handelsman J. 2022. THOR's hammer: the antibiotic koreenceine drives gene expression in a model microbial community. mBio 13:e0248621. https://doi.org/10. 1128/mbio.02486-21
- McCully Lucy M, Graslie J, McGraw AR, Bitzer AS, Sigurbjörnsdóttir AM, Vilhelmsson O, Silby MW. 2021. Exploration of social spreading reveals that this behavior is prevalent among *Pedobacter* and *Pseudomonas fluorescens* isolates and that there are variations in the induction of the phenotype. Appl Environ Microbiol 87:e0134421. https://doi.org/10. 1128/AEM.01344-21
- Filkins LM, Graber JA, Olson DG, Dolben EL, Lynd LR, Bhuju S, O'Toole GA. 2015. Coculture of Staphylococcus aureus with Pseudomonas aeruginosa drives S. aureus towards fermentative metabolism and reduced viability in a cystic fibrosis model. J Bacteriol 197:2252–2264. https://doi.org/10.1128/JB.00059-15
- Hotterbeekx A, Kumar-Singh S, Goossens H, Malhotra-Kumar S. 2017. In vivo and in vitro interactions between Pseudomonas aeruginosa and Staphylococcus spp. Front Cell Infect Microbiol 7:106. https://doi.org/10. 3389/fcimb.2017.00106
- Orazi G, O'Toole GA. 2017. Pseudomonas aeruginosa alters Staphylococcus aureus sensitivity to vancomycin in a biofilm model of cystic fibrosis infection. mBio 8:e00873-17. https://doi.org/10.1128/mBio.00873-17
- Waters VJ, Kidd TJ, Canton R, Ekkelenkamp MB, Johansen HK, LiPuma JJ, Bell SC, Elborn JS, Flume PA, VanDevanter DR, Gilligan P, Antimicrobial Resistance International Working Group in Cystic Fibrosis. 2019. Reconciling antimicrobial susceptibility testing and clinical response in antimicrobial treatment of chronic cystic fibrosis lung infections. Clin Infect Dis 69:1812–1816. https://doi.org/10.1093/cid/ciz364

September 2024 Volume 15 Issue 9 10.1128/mbio.00956-24**16** 

- Orazi G, Ruoff KL, O'Toole GA. 2019. Pseudomonas aeruginosa increases the sensitivity of biofilm-grown Staphylococcus aureus to membranetargeting antiseptics and antibiotics. mBio 10:e01501-19. https://doi. org/10.1128/mBio.01501-19
- Orazi G, Jean-Pierre F, O'Toole GA. 2020. Pseudomonas aeruginosa PA14 enhances the efficacy of norfloxacin against Staphylococcus aureus Newman biofilms. J Bacteriol 202:e00159-20. https://doi.org/10.1128/JB. 00159-20
- Hampton TH, Thomas D, van der Gast C, O'Toole GA, Stanton BA. 2021.
   Mild cystic fibrosis lung disease is associated with bacterial community stability. Microbiol Spectr 9:e0002921. https://doi.org/10.1128/ spectrum.00029-21
- Fischer AJ, Singh SB, LaMarche MM, Maakestad LJ, Kienenberger ZE, Pena TA, Stoltz DA, Limoli DH. 2021. Sustained coinfections with Staphylococcus aureus and Pseudomonas aeruginosa in cystic fibrosis. Am J Respir Crit Care Med 203:328–338.
- Emerson J, Rosenfeld M, McNamara S, Ramsey B, Gibson RL. 2002. Pseudomonas aeruginosa and other predictors of mortality and morbidity in young children with cystic fibrosis. Pediatr Pulmonol 34:91– 100. https://doi.org/10.1002/ppul.10127
- Zhao J, Schloss PD, Kalikin LM, Carmody LA, Foster BK, Petrosino JF, Cavalcoli JD, VanDevanter DR, Murray S, Li JZ, Young VB, LiPuma JJ. 2012. Decade-long bacterial community dynamics in cystic fibrosis airways. Proc Natl Acad Sci U S A 109:5809–5814. https://doi.org/10.1073/pnas. 1120577109
- Hubert D, Réglier-Poupet H, Sermet-Gaudelus I, Ferroni A, Le Bourgeois M, Burgel P-R, Serreau R, Dusser D, Poyart C, Coste J. 2013. Association between Staphylococcus aureus alone or combined with Pseudomonas aeruginosa and the clinical condition of patients with cystic fibrosis. J Cyst Fibros 12:497–503. https://doi.org/10.1016/j.jcf.2012.12.003
- Limoli DH, Yang J, Khansaheb MK, Helfman B, Peng L, Stecenko AA, Goldberg JB. 2016. Staphylococcus aureus and Pseudomonas aeruginosa co-infection is associated with cystic fibrosis-related diabetes and poor clinical outcomes. Eur J Clin Microbiol Infect Dis 35:947–953. https://doi. org/10.1007/s10096-016-2621-0
- Maliniak ML, Stecenko AA, McCarty NA. 2016. A longitudinal analysis of chronic MRSA and *Pseudomonas aeruginosa* co-infection in cystic fibrosis: a single-center study. J Cyst Fibros 15:350–356. https://doi.org/ 10.1016/i.icf.2015.10.014
- Chaney SB, Ganesh K, Mathew-Steiner S, Stromberg P, Roy S, Sen CK, Wozniak DJ. 2017. Histopathological comparisons of *Staphylococcus aureus* and *Pseudomonas aeruginosa* experimental infected porcine burn wounds. Wound Repair Regen 25:541–549. https://doi.org/10.1111/wrr. 12527
- Michelsen CF, Christensen A-MJ, Bojer MS, Høiby N, Ingmer H, Jelsbak L.
   2014. Staphylococcus aureus alters growth activity, autolysis, and antibiotic tolerance in a human host-adapted Pseudomonas aeruginosa lineage. J Bacteriol 196:3903–3911. https://doi.org/10.1128/JB.02006-14
- Castric PA. 1975. Hydrogen cyanide, a secondary metabolite of Pseudomonas aeruginosa. Can J Microbiol 21:613–618. https://doi.org/ 10.1139/m75-088
- Cox CD, Graham R. 1979. Isolation of an iron-binding compound from Pseudomonas aeruginosa. J Bacteriol 137:357–364. https://doi.org/10. 1128/jb.137.1.357-364.1979
- Hassan HM, Fridovich I. 1980. Mechanism of the antibiotic action pyocyanine. J Bacteriol 141:156–163. https://doi.org/10.1128/jb.141.1. 156-163.1980
- Cox CD, Adams P. 1985. Siderophore activity of pyoverdin for Pseudomonas aeruginosa. Infect Immun 48:130–138. https://doi.org/10. 1128/iai.48.1.130-138.1985
- Machan ZA, Taylor GW, Pitt TL, Cole PJ, Wilson R. 1992. 2-Heptyl-4hydroxyquinoline N-oxide, an antistaphylococcal agent produced by Pseudomonas aeruginosa. J Antimicrob Chemother 30:615–623. https:// doi.org/10.1093/jac/30.5.615
- Kessler E, Safrin M, Olson JC, Ohman DE. 1993. Secreted LasA of Pseudomonas aeruginosa is a staphylolytic protease. J Biol Chem 268:7503–7508.
- Cox CD, Rinehart KL, Moore ML, Cook JC. 1981. Pyochelin: novel structure of an iron-chelating growth promoter for *Pseudomonas aeruginosa*. Proc Natl Acad Sci U S A 78:4256–4260. https://doi.org/10.1073/pnas.78.7.4256

DeLeon S, Clinton A, Fowler H, Everett J, Horswill AR, Rumbaugh KP.
 2014. Synergistic interactions of *Pseudomonas aeruginosa* and *Staphylococcus aureus* in an *in vitro* wound model. Infect Immun 82:4718–4728. https://doi.org/10.1128/IAI.02198-14

- Beaudoin T, Yau YCW, Stapleton PJ, Gong Y, Wang PW, Guttman DS, Waters V. 2017. Staphylococcus aureus interaction with Pseudomonas aeruginosa biofilm enhances tobramycin resistance. NPJ Biofilms Microbiomes 3:25. https://doi.org/10.1038/s41522-017-0035-0
- Radlinski L, Rowe SE, Kartchner LB, Maile R, Cairns BA, Vitko NP, Gode CJ, Lachiewicz AM, Wolfgang MC, Conlon BP. 2017. Pseudomonas aeruginosa exoproducts determine antibiotic efficacy against Staphylococcus aureus. PLoS Biol 15:e2003981. https://doi.org/10.1371/ journal.pbio.2003981
- Lightbown JW, Jackson FL. 1956. Inhibition of cytochrome systems of heart muscle and certain bacteria by the antagonists of dihydrostreptomycin: 2-alkyl-4-hydroxyquinoline N-oxides. Biochem J 63:130–137. https://doi.org/10.1042/bj0630130
- Mitchell G, Séguin DL, Asselin A-E, Déziel E, Cantin AM, Frost EH, Michaud S, Malouin F. 2010. Staphylococcus aureus sigma B-dependent emergence of small-colony variants and biofilm production following exposure to Pseudomonas aeruginosa 4-hydroxy-2-heptylquinoline-Noxide. BMC Microbiol 10:33. https://doi.org/10.1186/1471-2180-10-33
- Fugère A, Lalonde Séguin D, Mitchell G, Déziel E, Dekimpe V, Cantin AM, Frost E, Malouin F. 2014. Interspecific small molecule interactions between clinical isolates of *Pseudomonas aeruginosa* and *Staphylococcus* aureus from adult cystic fibrosis patients. PLoS One 9:e86705. https://doi. org/10.1371/journal.pone.0086705
- Barraza JP, Whiteley M. 2021. A Pseudomonas aeruginosa antimicrobial affects the biogeography but not fitness of Staphylococcus aureus during coculture. mBio 12:e00047-21. https://doi.org/10.1128/mBio.00047-21
- Ibberson CB, Barraza JP, Holmes AL, Cao P, Whiteley M. 2022. Precise spatial structure impacts antimicrobial susceptibility of S. aureus in polymicrobial wound infections. Proc Natl Acad Sci U S A 119:e2212340119. https://doi.org/10.1073/pnas.2212340119
- Burrows LL. 2012. Pseudomonas aeruginosa twitching motility: type IV pili in action. Annu Rev Microbiol 66:493–520. https://doi.org/10.1146/ annurev-micro-092611-150055
- Limoli DH, Warren EA, Yarrington KD, Donegan NP, Cheung AL, O'Toole GA. 2019. Interspecies interactions induce exploratory motility in Pseudomonas aeruginosa. Elife 8:e47365. https://doi.org/10.7554/eLife. 47365
- 43. Yarrington KD, Shendruk TN, Limoli DH. 2024. The type IV pilus chemoreceptor PilJ controls chemotaxis of one bacterial species towards another. PLoS Biol 22:e3002488. https://doi.org/10.1371/journal.pbio. 3002488
- Wang GZ, Warren EA, Haas AL, Sánchez Peña A, Kiedrowski MR, Lomenick B, Chou TF, Bomberger JM, Tirrell DA, Limoli DH. 2023. Staphylococcal secreted cytotoxins are competition sensing signals for Pseudomonas aeruginosa. bioRxiv. https://doi.org/10.1101/2023.01.29. 526047
- Hartmann R, Jeckel H, Jelli E, Singh PK, Vaidya S, Bayer M, Rode DKH, Vidakovic L, Díaz-Pascual F, Fong JCN, Dragoš A, Lamprecht O, Thöming JG, Netter N, Häussler S, Nadell CD, Sourjik V, Kovács ÁT, Yildiz FH, Drescher K. 2021. Quantitative image analysis of microbial communities with BiofilmQ. Nat Microbiol 6:151–156. https://doi.org/10.1038/s41564-020-00817-4
- Limoli DH, Whitfield GB, Kitao T, Ivey ML, Davis MR, Grahl N, Hogan DA, Rahme LG, Howell PL, O'Toole GA, Goldberg JB. 2017. Pseudomonas aeruginosa alginate overproduction promotes coexistence with Staphylococcus aureus in a model of cystic fibrosis respiratory infection. mBio 8:e00186-17. https://doi.org/10.1128/mBio.00186-17
- Moormeier DE, Endres JL, Mann EE, Sadykov MR, Horswill AR, Rice KC, Fey PD, Bayles KW. 2013. Use of microfluidic technology to analyze gene expression during *Staphylococcus aureus* biofilm formation reveals distinct physiological niches. Appl Environ Microbiol 79:3413–3424. https://doi.org/10.1128/AEM.00395-13
- Turner KH, Wessel AK, Palmer GC, Murray JL, Whiteley M. 2015. Essential genome of *Pseudomonas aeruginosa* in cystic fibrosis sputum. Proc Natl Acad Sci U S A 112:4110–4115. https://doi.org/10.1073/pnas. 1419677112

- Cornforth DM, Diggle FL, Melvin JA, Bomberger JM, Whiteley M. 2020.
   Quantitative framework for model evaluation in microbiology research using *Pseudomonas aeruginosa* and cystic fibrosis infection as a test case. mBio 11:e03042-19. https://doi.org/10.1128/mBio.03042-19
- Aiyer A, Manos J. 2022. The use of artificial sputum media to enhance investigation and subsequent treatment of cystic fibrosis bacterial infections. Microorganisms 10:1269. https://doi.org/10.3390/ microorganisms10071269
- O'Toole GA, Kolter R. 1998. Flagellar and twitching motility are necessary for *Pseudomonas aeruginosa* biofilm development. Mol Microbiol 30:295–304. https://doi.org/10.1046/j.1365-2958.1998.01062.x
- Chiang P, Burrows LL. 2003. Biofilm formation by hyperpiliated mutants of *Pseudomonas aeruginosa*. J Bacteriol 185:2374–2378. https://doi.org/ 10.1128/JB.185.7.2374-2378.2003
- Conrad JC, Gibiansky ML, Jin F, Gordon VD, Motto DA, Mathewson MA, Stopka WG, Zelasko DC, Shrout JD, Wong GCL. 2011. Flagella and pilimediated near-surface single-cell motility mechanisms in *P. aeruginosa*. Biophys J 100:1608–1616. https://doi.org/10.1016/j.bpj.2011.02.020
- Whitchurch CB, Mattick JS. 1994. Characterization of a gene, pilU, required for twitching motility but not phage sensitivity in Pseudomonas aeruginosa. Mol Microbiol 13:1079–1091. https://doi.org/10.1111/j.1365-2958.1994.tb00499.x
- Stacy A, McNally L, Darch SE, Brown SP, Whiteley M. 2016. The biogeography of polymicrobial infection. Nat Rev Microbiol 14:93–105. https://doi.org/10.1038/nrmicro.2015.8
- Kim D, Barraza JP, Arthur RA, Hara A, Lewis K, Liu Y, Scisci EL, Hajishengallis E, Whiteley M, Koo H. 2020. Spatial mapping of polymicrobial communities reveals a precise biogeography associated with human dental caries. Proc Natl Acad Sci U S A 117:12375–12386. https://doi.org/ 10.1073/pnas.1919099117
- Wucher BR, Elsayed M, Adelman JS, Kadouri DE, Nadell CD. 2021.
   Bacterial predation transforms the landscape and community assembly of biofilms. Curr Biol 31:2643–2651. https://doi.org/10.1016/j.cub.2021. 03.036
- Krishna Kumar R, Meiller-Legrand TA, Alcinesio A, Gonzalez D, Mavridou DAI, Meacock OJ, Smith WPJ, Zhou L, Kim W, Pulcu GS, Bayley H, Foster

- KR. 2021. Droplet printing reveals the importance of micron-scale structure for bacterial ecology. Nat Commun 12:857. https://doi.org/10. 1038/s41467-021-20996-w
- Nadell CD, Drescher K, Foster KR. 2016. Spatial structure, cooperation and competition in biofilms. Nat Rev Microbiol 14:589–600. https://doi. org/10.1038/nrmicro.2016.84
- Winans JB, Wucher BR, Nadell CD. 2022. Multispecies biofilm architecture determines bacterial exposure to phages. PLoS Biol 20:e3001913. https://doi.org/10.1371/journal.pbio.3001913
- Wucher BR, Winans JB, Elsayed M, Kadouri DE, Nadell CD. 2023. Breakdown of clonal cooperative architecture in multispecies biofilms and the spatial ecology of predation. Proc Natl Acad Sci U S A 120:e2212650120. https://doi.org/10.1073/pnas.2212650120
- Oliveira NM, Wheeler JHR, Deroy C, Booth SC, Walsh EJ, Durham WM, Foster KR. 2022. Suicidal chemotaxis in bacteria. Nat Commun 13:7608. https://doi.org/10.1038/s41467-022-35311-4
- Korgaonkar AK, Whiteley M. 2011. Pseudomonas aeruginosa enhances production of an antimicrobial in response to N-acetylglucosamine and peptidoglycan. J Bacteriol 193:909–917. https://doi.org/10.1128/JB. 01175-10
- Mayer-Hamblett N, Rosenfeld M, Gibson RL, Ramsey BW, Kulasekara HD, Retsch-Bogart GZ, Morgan W, Wolter DJ, Pope CE, Houston LS, Kulasekara BR, Khan U, Burns JL, Miller SI, Hoffman LR. 2014. *Pseudomo-nas aeruginosa in vitro* phenotypes distinguish cystic fibrosis infection stages and outcomes. Am J Respir Crit Care Med 190:289–297. https://doi.org/10.1164/rccm.201404-0681OC
- Hmelo LR, Borlee BR, Almblad H, Love ME, Randall TE, Tseng BS, Lin C, Irie Y, Storek KM, Yang JJ, Siehnel RJ, Howell PL, Singh PK, Tolker-Nielsen T, Parsek MR, Schweizer HP, Harrison JJ. 2015. Precision-engineering the Pseudomonas aeruginosa genome with two-step allelic exchange. Nat Protoc 10:1820–1841. https://doi.org/10.1038/nprot.2015.115
- Bose JL, Lehman MK, Fey PD, Bayles KW. 2012. Contribution of the Staphylococcus aureus Atl AM and GL murein hydrolase activities in cell division, autolysis, and biofilm formation. PLoS One 7:e42244. https://doi.org/10.1371/journal.pone.0042244